First-principles calculations of the structural and electronic properties of the ScN(001) surface

Noboru Takeuchi

*Centro de Ciencias de la Materia Condensada, Universidad Nacional Autónoma de México, Apartado Postal 2681, Ensenada,
Baja California, 22800, México*

Sergio E. Ulloa

Department of Physics and Astronomy, and Condensed Matter and Surface Sciences Program, Ohio University, Athens, Ohio 45701
(Received 28 January 2002; published 28 May 2002)

We have studied the structural and electronic properties of the (001) surface of ScN by first-principles total-energy calculations. Since experimental scanning tunneling microscope (STM) images indicate a (1×1) periodicity, we have restricted our calculations to models compatible with this periodicity. Several structures were considered in our study. It was found that for a N-rich surface, the most stable configuration corresponds to a relaxed bulk terminated surface. Electronic properties of this surface are similar to those of the bulk and the surface is *semiconductor*. In contrast, the most favorable configuration for a Sc-rich surface corresponds to a surface with N vacancies in the first layer. In this case the surface is *metallic*. Our calculations, and predicted bias dependence of STM images, are in good agreement with experiments.

I. INTRODUCTION

Group IIIA nitrides such as GaN and AlN, with excellent physical properties, including hardness and high-temperature stability, have been extensively studied[1–7] because they are important technological materials.[8] These materials are wide band-gap semiconductors, and crystallize in either the zincblende or the wurtzite structure. The difference in total energy between these two phases is very small and sometimes both of them can be obtained experimentally. Wurtzite and zincblende are structurally similar (they differ only by the stacking in the (111) direction, and atomic coordination in either zincblende or wurtzite is exactly the same through the second neighbor). On the other hand, the ground-state structure of group IIIB nitrides, such as ScN, and other transition-metal nitrides, is rock salt (NaCl). These materials can be either metal or semiconductor.[9]

Very recently, smooth epitaxial growth of singly oriented ScN films was achieved, demonstrating the possibility of using ScN as an electronic material. ScN is believed to be a narrow gap semiconductor (with a fundamental indirect gap of ~0.9–1.6 eV) and since its lattice constant is very similar to GaN (a wide-gap semiconductor),[10–12] combining the two semiconductors in the form of heterostructures could be useful in the fabrication of electronic devices. Smith and co-workers have reported the growth of ScN smooth films using radio frequency molecular-beam epitaxy.[13,14] They have found well oriented ScN films grown in either the (001), (110), or (111) orientation, depending on the starting substrate. They also observed that the growth in the (110) and (111) orientations was in three dimensions and forming rough surfaces. On the other hand, the growth in the (001) orientation was two dimensional, and it resulted in atomically smooth surfaces. Reflection high-energy electron-diffration patterns for the ScN(001) surface show a (1×1) symmetry. This result was confirmed by (STM) images of the surface showing atomic resolution: the square (1×1) periodicity is clearly seen in those images. However, only

one of the two sublattices (Sc or N) was observed. An ideally bulk terminated (001) plane contains the two kinds of atoms in a fcc configuration. Since the STM image was taken at a negative sample bias of -0.5 V (indicating that they are looking at occupied states), Al-Brithen and Smith suggested that they were imaging *N* atoms. However, dual bias images obtained at ± 1 V showed a very small shift, less than the expected a/2, indicating that they were observing the same atoms at both polarities. In a following paper, Smith *et al.* reported a study of the growth of ScN epitaxial layers for different Sc/N flux ratios. They found this flux ratio to be critical to the structural, optical, and electronic properties of the films. Two different regimens were found in their experiments. Under N-rich conditions, the growth was epitaxial, the films were stoichiometric and transparent with a direct optical transition at 2.15 eV. Since first-principles calculations and optical experiments have found a direct optical transition in the range of 2.1–2.4 eV for bulk ScN,[10,15–18] this result is an indication that the surface electronic structure is similar to the one of bulk ScN. Under Sc-rich conditions the growth is also epitaxial, but the Sc excess leads to the formation of N vacancies. There is also a drop in electrical resistivity, and an optical reflection edge at 1 eV, well below the 2.15 eV band gap, suggesting the presence of free carriers (metallic behavior) in the films.

In this paper, we present first-principles total-energy calculations of the (001) surface of ScN. Different structures having different number of surface atoms were optimized. As in the experiment, our calculations show two different regimens. The most stable configuration for a N-rich surface corresponds to a relaxed bulk terminated surface. Electronic properties are similar to those of the bulk and the surface is semiconductor. For a Sc-rich surface, the most favorable configuration corresponds to a surface with N vacancies in the first layer. In this case the surface is metallic. Our calculations are then in total qualitative agreement with experiments.

We discuss moreover the relation of the N-rich surface

structure with the bias dependence of the STM imaging. We show that at ± 1 V from the *unbiased* Fermi level, one would indeed expect to observe different atoms (N or Sc) on the images. The results indicate that a small doping shifting the Fermi level is present in the samples, and suggest that dual bias images over a larger range would yield the anticipated sublattice images.

II. METHOD

The calculations were performed in the framework of density-functional theory. We have employed the full-potential linearized augmented plane-wave method as implemented in the WIEN97 code.[19] The exchange and correlation effects were treated using the generalized gradient approximation (GGA).[20] We have used a repeated slab geometry in order to describe the surfaces. Each slab consists of five atomic (001) planes with one Sc and one N atom in a (1$\times$1) configuration. The calculated bulk lattice constant of 4.54 Å was used in the calculations. In these systems, there are two different (001) surfaces: one at the top of the slab and the other at the bottom. To decouple two consecutive slabs, we have separated them by a vacuum region of $\sim$9 Å, corresponding to four atomic layers. We have used 10 k points in the irreducible part of the surface Brillouin zone (SBZ). A larger mesh of 21 k points in the irreducible part of the SBZ was used in selected calculations. Differences in total energies changed by less that 1 meV/[(1$\times$1) cell] and atomic coordinates changed by less than 0.003 Å.

III. SURFACE FORMATION ENERGIES

We have first determined the optimal geometry of the (001) surface of ScN according to four different models, each one having a (1$\times$1) periodicity. The first one corresponds to an ideally bulk terminated surface. The second and third models correspond to a surface in which N or Sc atoms are missing from the first layer. In the last model, we consider the possibility of the N vacancies moving into the second layer. Since, the four structures contain different number of atoms, we cannot compare directly their total energies. Instead, we have to use the surface formation energy, defined in terms of the thermodynamic potential,

$$\Omega = E_{slab}(n_{Sc},n_N) - TS - n_{Sc}\mu_{Sc} - n_N\mu_N,$$

where $E_{slab}(n_{Sc},n_N)$ is the total energy of the ScN system, n_{Sc} and n_N are the number of Sc and N atoms, μ_{Sc} and μ_N are the chemical potentials of Sc and N, respectively. The entropy term TS is assumed to contribute very little to the differences in Ω for the various structures, and it is, therefore, neglected. The surface formation energy E_s is equal to $\Omega/2A$, where the 1/2 factor comes from the two surfaces that we have in our slab. A is the surface area, which in the present case is the same for all the structures, and it corresponds to the (1$\times$1) unit cell. The sum of the N and Sc chemical potentials is constrained to be equal to the energy per unit cell in bulk ScN: $\mu_{Sc} + \mu_N = \mu_{ScN(bulk)}$. In addition, $\mu_{Sc} \lesssim \mu_{Sc(bulk)}$, and $\mu_N \lesssim \mu_{N(bulk)}$, otherwise a bulk Sc or a
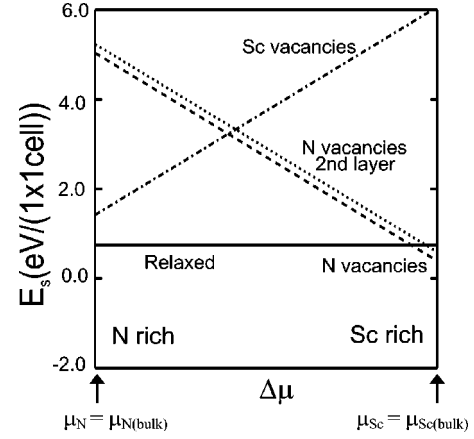

FIG. 1. Surface formation energies for several models of the ScN(001) surface as function of the difference in chemical potentials for Sc and N, $\Delta\mu = \mu_{Sc} - \mu_N$. The lower limit for $\Delta\mu$ corresponds to $\mu_N = \mu_{N(bulk)}$ and the upper limit to $\mu_{Sc} = \mu_{Sc(bulk)}$. Solid, horizontal line corresponds to the simply relaxed surface, with the lowest energy but near $\mu_{Sc} \simeq \mu_{Sc(bulk)}$.

bulk N would precipitate. These three equations limit the allowed values of their difference $\Delta\mu = \mu_{Sc} - \mu_N$ in the following way:

$$\mu_{Sc(bulk)} - \mu_{N(bulk)} - \Delta H < \Delta\mu < \mu_{Sc(bulk)} - \mu_{N(bulk)} + \Delta H,$$

where $\Delta H = \mu_{Sc(bulk)} + \mu_{N(bulk)} - \mu_{ScN(bulk)}$ is the heat of formation of bulk ScN from bulk Sc and bulk N.

One can then write down the surface formation energy E_s in function of $\Delta\mu$ as

$$E_s = \frac{1}{2A}\left\{ E_{slab}(n_{Sc},n_N) - \frac{1}{2}(n_{Sc}+n_N)\mu_{ScN(bulk)} \right.$$
$$\left. - \frac{1}{2}(n_{Sc}-n_N)\Delta\mu \right\}.$$

The surface formation energies of the calculated phases are plotted in Fig. 1 as a function of $\Delta\mu$ over the permitted range of $2\Delta H$. Two different growth regimens can be observed. For most of the allowed range of $\Delta\mu$, the most stable configuration corresponds to the relaxed bulk terminated structure (solid, horizontal curve). However, if the Sc chemical potential is near is maximum, $\mu_{Sc} \simeq \mu_{Sc(bulk)}$, and the N chemical potential is low, then the structure with N vacancies becomes more stable (dashed curve). This is in very good agreement with the experimental results of Smith *et al.* Our results also show that the structure in which the N vacancies move to the second layer differs by only 0.2 eV/[(1$\times$1) cell] from the structure with vacancies in the first layer. This is an indication that N vacancies can be incorporated very easily in the ScN film, maintaining in this way the rock-salt structure.

IV. STRUCTURAL PROPERTIES

In this section, we present the structural properties of the two stable surfaces of ScN(001). The first one corresponds to the N-rich configuration: the relaxed bulk terminated struc-
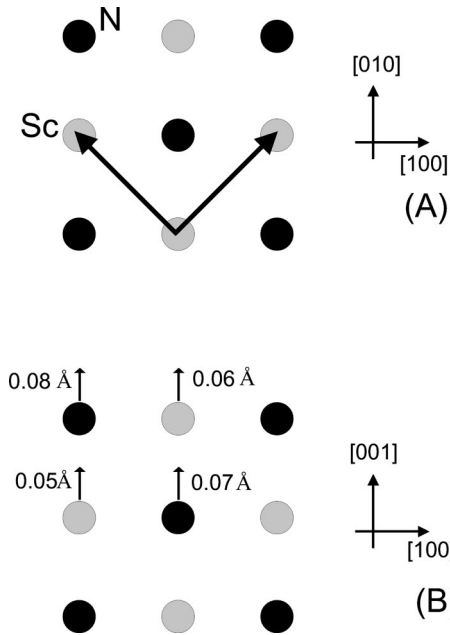
FIG. 2. Schematic view of the simply relaxed ScN (001) surface. (a) Top view, (b) side view.

FIG. 3. Schematic view of the ScN (001) surface with N vacancies in the first layer. (a) Top view, (b) side view.

ture. Figures 2(a) and 2(b) shows schematically the fully relaxed atomic positions. It can be observed that atoms hardly move from their original bulk sites. This result is not surprising, since the ionic character in the bonding of the rock-salt structure tends to suppress charge transfers, and it, therefore, prevents drastic changes in the surface. First layer Sc and N atoms are pushed up by 0.06 and 0.08 Å, respectively. Therefore, the relative buckling between the Sc and N atoms in the first layer is 0.02 Å, with the N atoms being further up. The energy gain associated with the surface relaxation is rather small: 0.03 eV/[(1×1) cell].

The second structure corresponds to the end of the Sc-rich regimen: a surface in which all N atoms are missing from the first layer. Results are summarized in Figs. 3(a) and 3(b) . In this case, and somewhat surprising, only one kind of atom has a significant displacement from a bulk terminated structure: N atoms in the second layer are pushed up by 0.16 Å. Sc atoms in the first layer move up by only 0.02 Å, while Sc atoms in the second layer move in the other direction by 0.03 Å .

V. ELECTRONIC PROPERTIES

In this section, we study the electronic properties of the (001) surface of ScN. We have first considered the simple relaxed surface. Figure 4(a) shows the local density of states (LDOS) of the slab. It is very similar to the LDOS of bulk ScN, showing a very small (or nearly zero) gap. Our calculations have been performed with the GGA approximation and, therefore, in similarity with bulk ScN, we expect the gap to be larger and the surface to be semiconductor. Three main regions can be observed in this figure: one between -14 and -12 eV, another between -5 eV and the Fermi level, and the last one in the empty states region, between the Fermi level and around 10 eV. To clearly identify these peaks, we
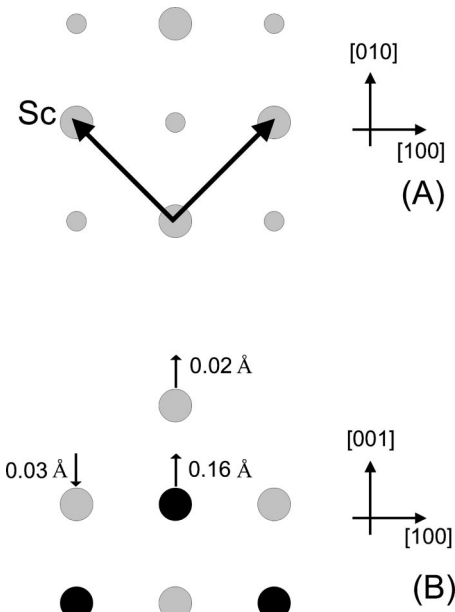
present in Figs. 4(b) and 4(c) partial density of states. Figure 4(b) corresponds to the first layer Sc atom, while Fig. 4(c) corresponds to the first layer N atom. It can be observed that the feature between -14 and -12 eV is mainly due to N $2s$ electrons, and the peak between -5 and 0 eV to N $2p$ electrons, with a small contribution from Sc $3d$ electrons. The peak above the Fermi level has the biggest contribution from Sc $3d$ electrons and a smaller contribution from the other electrons. The behavior of the LDOS of this surface is very similar to the one in bulk ScN.[11] It basically shows the ionic character of the bonding.

A drastically different situation is obtained in the structure with N vacancies in the Sc-rich regime (Fig. 5). The surface becomes metallic, as the general shape of the LDOS is maintained with respect to the relaxed bulk structure, but with the introduction of new peaks close to the Fermi level in the gap. With the absence of the first layer N atoms, the metallic behavior of first layer Sc atoms is in someway recovered. Experimental results of Smith *et al.* show that there is a reduction in the resistivity of the surface, indicating that in the Sc-rich regime the surface is more metallic. However, they still observed the direct absorption at 2.15 eV. In our calculations, we are assuming no nitrogen atoms in the first layer. In the experiments, some of the Nitrogen atoms in the first layer are missing, but probably not all. Also, there are N vacancies inside the film. Our calculations have shown that the difference in energy between vacancies in the first layer and vacancies in the second layer is very small.

VI. SIMULATED STM IMAGES OF THE N-RICH SURFACE

Since the LDOS of the N-rich surface is dominated by N $2p$ electrons below the Fermi level, and by Sc $3d$ electrons above, we may think that N (Sc) atoms should be visible at negative (positive) sample polarities in STM images. How-
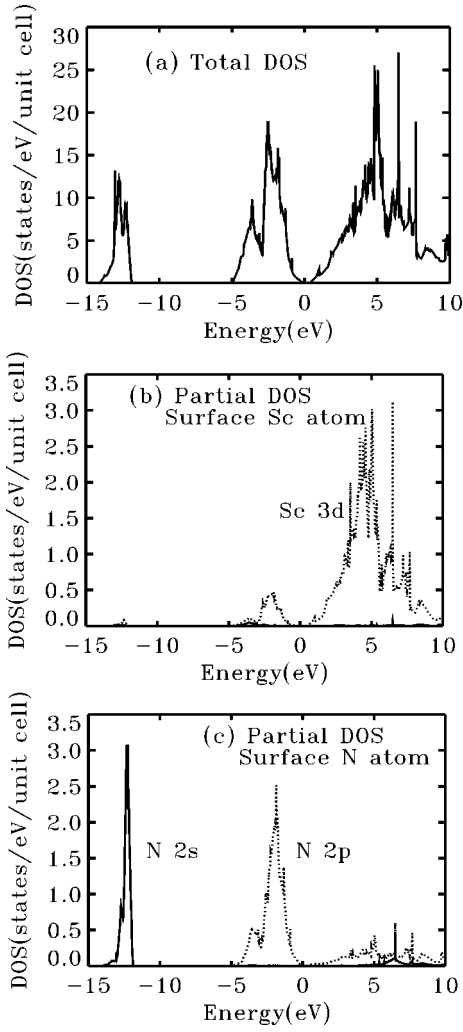
FIG. 4. Density of States for the relaxed ScN(001) surface. (a) Total, (b) partial, corresponding to first layer Sc atoms, and (c) partial, corresponding to first layer N atom.

ever, in the experiments of Smith *et al.*, dual bias images obtained at ± 1 V showed a very small shift, less than a/2, indicating that they were observing the same atoms at both polarities. To compare our results with the experimental STM images, we approximate the theoretical tunneling current density $j(\mathbf{r})$ by[21]
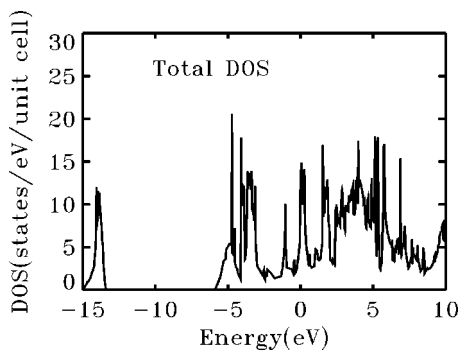

FIG. 5. Total density of states for the ScN(001) surface with first layer of N atoms missing from the surface.
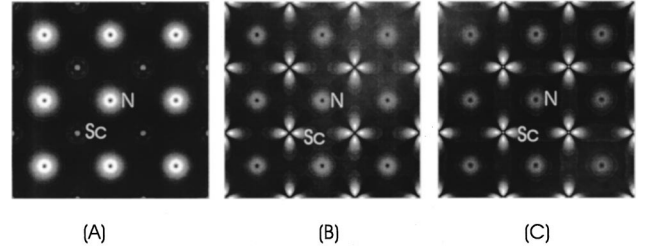

FIG. 6. Gray plots of the local density of states for the N-rich surface (a) $V \sim -1.0$ V, (b) $V \sim -0.5$ V, and (c) $V = +1.0$ V.

$$j(\mathbf{r}, V) \propto \int_{E_F - eV}^{E_F} \rho(\mathbf{r}, E) dE,$$

where

$$\rho(\mathbf{r}, E) \equiv \sum_{n, \mathbf{k}} |\psi_{n, \mathbf{k}}(\mathbf{r})|^2 \delta(E_{n, \mathbf{k}} - E).$$

Here $\rho(\mathbf{r}, E)$ is the local density of states at the tip position $\mathbf{r} = (x, y, z)$, and the $\psi_{n, \mathbf{k}}(\mathbf{r})$ are the eigenstates of the surface with corresponding energy $E_{n, \mathbf{k}}$. We integrate the charge density of the ScN(001) surface using Eq. (1) with $z \sim 2$ Å, and $V = -1.0, -0.5,$ and 1.0 V. In the simplest approximation, this corresponds to the experimental procedure of probing surface states at a negative bias voltage of -1.0 V, -0.5 V, and positive bias voltages of 1.0 V, respectively.

At $V = -1.0$ V, the brightest features originate from N atoms [Fig. 6(a)], while at $V = -0.5$ V [Fig. 6(b)] and $V = +1.0$ V [Fig. 6(c)] they correspond to Sc atoms (more specifically to their d electrons). These results suggest a natural explanation to the experiments showing the same kind of atoms in STM images at opposite polarities. Indeed, if one considers that a slight p doping exists in the samples (in agreement with the observations of Smith *et al.*), one can expect that the real Fermi level has been shifted by 0.5 V or so, and that the ± 1 V images would yield only images similar to those shown here in Figs. 6(a) and 6(b). It would be interesting if STM experiments could be performed with larger voltages of around ± 5 V in the dual bias images. At these voltages, our calculations clearly predict that at negative sample bias voltages mostly N atoms should be visible, while at positive sample bias voltages, Sc atoms should dominate the images. Notice, incidentally, that the four-leaf symmetry of the Sc atoms (its d electrons) is evident in Fig. 6(c) (although hardly distinguishable in experiments).

VII. SUMMARY

In this paper we have performed first-principles total-energy calculations of the ScN(001) surface. Different structures with periodicity (1×1) were fully optimized. Calculations of the surface formation energies indicate two different growth regimens. For N-rich surfaces, our calculations favor a simply relaxed bulk terminated surface. There is a very small buckling between the first layer Sc and N atoms, with

the N atoms being pushed 0.02 Å further up. Electronic properties are similar to those of the bulk and the surface is semiconductor. For a Sc-rich surface, the most favorable configuration corresponds to a surface with N vacancies in the first layer. In this case the surface is metallic. Our calculations are in good agreement with experiments.

[1] W.M. Yim and R.J. Paff, J. Appl. Phys. **45**, 1456 (1974).

[2] P.E. Van Camp, V.E. Van Doren, and J.T. Devreese, Phys. Rev. B **44**, 9056 (1991).

[3] V.A. Tyagi, A.M. Evstigneev, A.N. Krasiko, A.F. Malakhov, and V. Ya, Sov. Phys. Semicond. **11**, 1257 (1977).

[4] P.E. Van Camp, V.E. Van Doren, and J.T. Devreese, Solid State Commun. **81**, 23 (1992).

[5] A. Munoz and K. Kunc, Phys. Rev. B **44**, 10 372 (1991).

[6] B.J. Min, C.T. Chan, and K.M. Ho, Phys. Rev. B **45**, 1159 (1992).

[7] C.-Y Yeh, Z.W. Lu, S. Froyen, and A. Zunger, Phys. Rev. B **46**, 10 086 (1992).

[8] S. Nakamura, Solid State Commun. **102**, 237 (1997).

[9] C. Stampfl, W. Mannstadt, R. Asahi, and A. Freeman, Phys. Rev. B **63**, 155106 (2001).

[10] W.R.L. Lambrecht, Phys. Rev. B **62**, 13 538 (2000).

[11] N. Takeuchi, Phys. Rev. B **65**, 045204 (2002).

[12] R. Monnier, J. Rhyner, T.M. Rice, and D.D. Koelling, Phys. Rev. B **31**, 5554 (1985).

[13] H.A. Al-Brithen and A.R. Smith, Appl. Phys. Lett. **77**, 2485 (2000).

[14] A.R. Smith, H.A.H. Al-Brithen, D.C. Ingram, and D. Gall, J. Appl. Phys. **90**, 1809 (2001).

[15] P. Dismukes, W.M. Yim, and V.S. Ban, J. Cryst. Growth **13/14**, 365 (1972).

[16] D. Gall, I. Petrov, L.D. Madsen, J.-E Sundgren, and J.E. Geene, J. Vac. Sci. Technol. A **16**, 2411 (1998).

[17] D. Gall, I. Petrov, N. Hellgren, L. Hulman, J.-E Sundgren, and J.E. Geene, J. Appl. Phys. **84**, 6034 (1998).

[18] T.D. Moustakas, R.J. Molna, and J.P. Dismukes, Electrochem. Soc. Proc. **96-11**, 197 (1996).

[19] P. Blaha, K. Schwarz, and J. Luitz, Computer code WIEN97, A Full Potential Linearized Augmened Plane Wave Package for Calculating Crystal Properties (Karlheinz Schwarz, Technical Universität Wien, Austria, 1999).

[20] J.P. Perdew, K. Burke, and M. Ernzerhof, Phys. Rev. Lett. **77**, 3865 (1996).

[21] A. Selloni, P. Carnevali, E. Tosatti, and C.D. Chen, Phys. Rev. B **31**, 2602 (1985).